CHALMERS
UNIVERSITY OF TECHNOLOGY

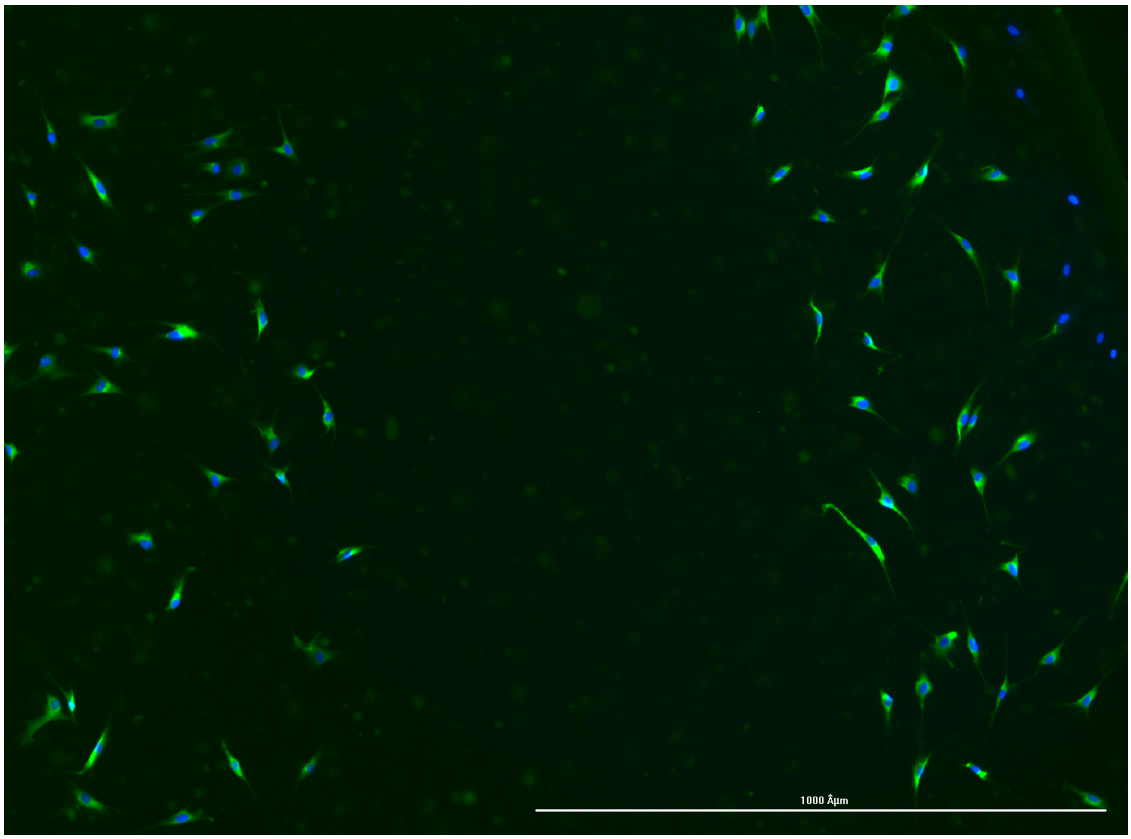

Senescence in Skin Aging

Quantifying methods and anti-aging treatments

Master's Thesis in Biotechnology

YLVA ÖBERG

DEPARTMENT OF LIFE SCIENCES
CHALMERS UNIVERSITY OF TECHNOLOGY
Gothenburg, Sweden 2024
www.chalmers.se

Master's thesis 2024

Senescence in Skin Aging

Quantifying methods and anti-aging treatments

YLVA ÖBERG

CHALMERS
UNIVERSITY OF TECHNOLOGY

Department of Life Sciences
Chalmers University of Technology
Gothenburg, Sweden 2024

Senescence in Skin Aging
Quantifying methods and anti-aging treatments
YLVA ÖBERG

Supervisor: Christina Österlund, PhD, Oriflame Cosmetics
Examiner: Anette Larsson, PhD, Department of Applied Chemistry

Master's Thesis 2024
Department of Life Sciences
Chalmers University of Technology
SE-412 96 Gothenburg
Telephone +46 31 772 1000

Cover: Fluorescent Microscopic picture with 20x objective of C12FDG-stained Human Dermal Fibroblasts.

Typeset in LaTeX
Printed by Chalmers Reproservice
Gothenburg, Sweden 2024

Senescence in Skin Aging
Quantifying methods and anti-aging treatments
YLVA ÖBERG
Department of Life Sciences
Chalmers University of Technology

Abstract

Aging is characterized by gradual and continuous deterioration of physiological functions over time. Aging research explores the underlying cellular mechanisms and genetic pathways involved in the decline, with the final goal of therapeutic and cosmetic interventions for age-related alterations and pathologies. Senescence has been identified as a central hallmark of aging. With age, our immune system and DNA damage repair mechanisms become less efficient, resulting in an accumulation of senescent cells. They cease to proliferate and grow, irreversibly exit the cell cycle, thus causing a loss of genome integrity. The development of anti-aging interventions relies substantially on research into methods to measure and explore the underlying mechanisms of senescence.

To understand the process of skin aging, this study is looking at cellular senescence, with special emphasis on replicative-induced senescence in Human Dermal Fibroblasts. In the quest for multiple tools to objectively measure cellular senescence in this cell model, an in-vitro cell-based model was developed based on established quantifying methods: NAD+/NADH-Glokit, Quantitative Real-Time PCR (qPCR), Flow Cytometry, SA-β-Galactosidase staining and Immunofluorescence for C12FDG. The assays included in the proposed model were validated by demonstrating a statistically significant difference between high and low-passage HDFs. The model is a good starting point to objectively quantify cellular senescence in skin-aging research. However, the model at this stage does not describe the senescent phenotype in its full complexity; more biomarkers need to be taken into account. Research is ongoing and further research is needed to expand the tools in the toolbox.

Furthermore, this study applied the NAD+/NADH ratio of the model to test the effects certain flavonoid treatments (Quercetin, Apigenin and Kaempferol) have on skin senescence modulation, as compared to the chemical 78c treatment proven to reverse age-associated metabolic decline. Only treatment with low concentrations of Apigenin successfully increased the NAD+/NADH ratio in high-passage cells. However, further research is needed to confirm the results of the limited sample size in this study and to draw any steadfast conclusions.

Keywords: skin aging, replicative-induced senescence, aging research, assay, human dermal fibroblasts, skin senescence modulation, NAD+/NADH-Glo™assay, RT-qPCR, SA-β-Galactosidase staining, C12FDG, flow cytometry, 78c, Quercetin, Apigenin, Kaempferol.

Acknowledgements

I extend my deepest gratitude to Dr. Christina Österlund, my supervisor at Oriflame Cosmetics, whose expert guidance and unwavering support have made the completion of this thesis project possible. I am also deeply thankful to Nina Hrapovic, Ines Martin, Dr. Lene Visdal-Johnsen and the entire team at Oriflame Cosmetics for their generous assistance, expert advice, and for providing all necessary equipment and materials. The collaborative spirit at Oriflame has truly enriched my learning experience. Special thanks to my examiner, Prof. Dr. Anette Larsson, for her guidance and support throughout this journey.

Ylva Öberg, Gothenburg, June 2024

List of Acronyms

Below is the list of acronyms that have been used throughout this thesis listed in alphabetical order:

78c	Compound 78
β-Gal	β-Galactosidase
ATP	Adenosine Triphosphate
C12FDG	5-Dodecanoylaminofluorescein Di-Beta-D-Galactopyranoside
CD38	Cluster of Differentiation 38
CDK	Cyclin-Dependent Kinase
CDKN1A	Gene encoding p21 protein
CDKN2A	Gene encoding p16 protein
cDNA	Complementary Deoxyribonucleic Acid
DAPI	4'-6-Diamidino-2-Phenylindole, Dihydrochloride
DMEM	Dulbecco's Modified Eagle Medium
DNA	Deoxyribonucleic Acid
DTAB	Dodecyltrimethylammonium Bromide
ELISA	Enzyme-Linked Immunosorbent Assay
FBS	Fetal Bovine Serum
GAPDH	Glyceraldehyde 3-Phosphate Dehydrogenase
HDF	Human Dermal Fibroblast
IL	Interleukin
LMNB1	Gene encoding Lamin-B1 protein
MMP	Matrix Metalloproteinase
NAMPT	Nicotinamide Phosphoribosyltransferase
NAD/NADH	Nicotinamide Adenine Dinucleotide
p16	Protein involved in cell cycle arrest
p21	Tumor suppressor protein, induced by p53
p53	Tumor suppressor protein
PBS	Phosphate-Buffered Saline
PEST	Penicillin-Streptomycin
qPCR	Quantitative Polymerase Chain Reaction
RIS	Replicative-Induced Senescence
RNA	Ribonucleic Acid
SA	Senescence-Associated
SASP	Senescence-Associated Secretory Phenotype
SIRTs	Sirtuin family enzymes
TP53	Gene encoding p53 protein
UT	Untreated

Contents

List of Figures

List of Tables

1
Introduction

Physical aging of the skin is caused by internal and external factors [1]. Intrinsic aging of the skin is the inevitable physiological process that results in thin, dry skin, fine wrinkles and gradual dermal atrophy, while extrinsic aging is engendered by external environmental factors such as air pollution, smoking, poor nutrition and sun exposure, resulting in coarse wrinkles, loss of elasticity, laxity and rough-textured appearance [2].

Research into aging from a broader perspective experienced an unprecedented growth with over 300 000 publications on the topic in the last decade only [3]. In fact, aging research is immediately relevant to understand a wide range of age-related pathologies, including pruritus, metabolic disorders and cancer [4][5]. A landmark review article by Carlos López-Otin et al. [3] enumerates twelve hallmarks that drive aging, incorporating evidence from the latest aging research on molecular, cellular and systemic processes that account for age-associated alterations. These hallmarks of aging are defined in terms of their manifestation, as well as the possibility to accelerate and, more importantly, decelerate, halt or reverse aging by therapeutic interventions. Each of these hallmarks is a starting point for further research to objectively quantify the aging process, specifically at the single-cell level.

Senescence is one of these key hallmarks that drive aging. Senescence occurs when cells undergo an irreversible growth arrest and cease to divide. The cellular mechanisms underlying senescence are very complex. Organisms have a sophisticated DNA repair mechanism, in which cells identify and correct damage to nuclear and mitochondrial DNA caused over time by internal and external stresses [6]. These repair mechanisms are crucial for maintaining genome integrity and for preventing the accumulation of genomic damage. However, as we age, these repair mechanisms become less effective, putting the genome integrity at risk. The genetic damage and a wide range of defects (e.g. mutations, deletions, single- or double-strand breaks) [7], together with its cytosolic buildup, causes senescence in cells. Senescence can accelerate age-related dysfunction in dermal cells; the breakdown of collagen and elastin can lead to wrinkles, a sagging appearance and other visible signs of aging [8]. Strategies to target senescent cells are therefore interesting to investigate for their potential in preventing skin aging.

The underlying mechanisms of cellular senescence are not, as yet, fully understood. The pursuit of innovative solutions to defy or even reverse skin aging is a topic of major interest also for the skin care and cosmetics industries. The global anti-aging

market is projected to reach US$ 120 billion by 2030 [9]. Oriflame Cosmetics is an international cosmetics company that is actively engaged in anti-aging research, currently pursuing studies into the main cellular mechanisms associated with aging. This Master's thesis is conducted under the umbrella of Oriflame Cosmetics, with the aim to develop an in-vitro cell-based model quantifying replicative-induced senescence.

2
Aim

The aim of this project is to develop an in-vitro cell-based model quantifying replicative-induced senescence, with the further aim to monitor the effects on senescence of some naturally-derived compounds and extracts.

2.1 Clarification of Research Question

The aim of the project is to create a model based on standardized methods from literature to quantify replicative-induced senescence in Human Dermal Fibroblasts (HDFs). In addition, the study aims to expose cells to different treatments with naturally-derived compounds shown in literature to counteract senescence and measure their effects on the senescent phenotype, using and validating the newly developed model.

Standardized methods designed to detect specific markers of senescence include NAD+/NADH assay, qPCR, flow cytometry, SA-β-Galactosidase staining and Immunofluorescence for C12FDG. These established methods are applied to a cell model consisting of replicative-induced senescence in Human Dermal Fibroblasts (HDFs). Replicative-induced senescence of Human Fibroblasts is a widely used cellular model for human aging. Conducting research on replicative-induced senescence in vitro is described in the literature as simulating intrinsic aging. Each assay is validated if it is able to detect statistically significant differences between cells in high (old) and low (young) passage.

Furthermore, the NAD+/NADH assay if validated is used as a tool to objectively measure whether treatments have an impact on the senescent phenotype. The aim is to test treatments with naturally-derived compounds. Quercetin, Apigenin and Kaempferol are naturally-derived extracts that in literature have been shown to successfully treat senescence in vivo and/or in vitro. 78c is a prime candidate to provide positive control of senescence treatments. It is a chemical treatment proven to reverse age-associated metabolic decline.

2.2 Limitations

The experiments are conducted solely on mono-cultured primary Human Dermal Fibroblast cells. Due to ethical reasons, no animal models are used in the experiments. Ex-vivo testing is exclude because of time limitations.

Only replicative-induced senescence is studied, which simulates intrinsic aging. Consequently, extrinsic aging is excluded from the scope of this study, as are other relevant hallmarks of aging like autophagy. They are not a part of this study at this time.

Because of a growing interest in naturally-derived cosmetic products, this study investigates flavonoids as potential treatments for senescence, excluding treatments with synthetic compounds. The synthetic compound 78c is tested but only as a candidate to provide positive control of senescence treatments. More importantly, to measure the impact of flavonoid treatments on the senescent phenotype, only the NAD+/NADH assay was used, as this assay was prioritized by Oriflame Cosmetics as the most interesting for evaluating treatments, and due to time limitations of the study.

3
Theory

After a brief introduction into the cellular context for skin aging research (3.1 Skin anatomy, skin aging and Human Dermal Fibroblasts), this section will discuss the following questions: what is cellular senescence (3.2 Cellular senescence), how to detect cellular senescence (3.3 Detection methods for senescence), and how to treat cellular senescence (3.4 Treatments to combat senescence). The content for this literature study was primarily retrieved from databases provided by Chalmers Library, along with other sources provided by Oriflame Cosmetics.

3.1 Skin anatomy, skin aging and Human Dermal Fibroblasts

To gain a deeper understanding of what occurs during skin aging, it is essential to comprehend the anatomy of the skin, the function of its constituents, and how these change throughout life. The skin is the largest human organ, often described as the frontline defense, the barrier protecting the body from pathologies. The three main layers of the skin are (from outward to inward) the epidermis, dermis and hypodermis. They each have their own distinct structure, function and cellular composition.

This study looks at Human Dermal Fibroblasts (HDFs), a cell type located in the dermis that is relevant when talking about skin aging. Though collagen is the primary component of the dermis, fibroblasts are the principle cellular population of the dermis, responsible for maintaining the structure. One of the many functions of fibroblasts is to synthesize collagen, elastic and reticular fibers [10][11]. This explains why healthy fibroblasts are crucial for maintaining healthy skin with youthful appearance. In aging skin, the number of fibroblasts decreases and their functioning is compromised. Subsequently, collagen production is suppressed and collagen degradation exacerbated, which in turn leads to visual signs of aging [12]. In addition, fibroblasts in aging skin display decreased growth factor response and increased superfluous proteolytic activity, which further accelerates the aging process [13].

Fibroblasts are widely used and well-established in the literature studying senescence in vitro [11]. They are susceptible to age-associated alterations when exposed to stress. Unlike immortalized cell lines that proliferate indefinitely, primary fibroblasts with their finite number of divisions are more suited to mimic the in-vivo aging process. Moreover, they are easy and inexpensive to grow and culture. As the same cell type is used in a lot of research, findings are more easily comparable as well.

There are many different ways to trigger senescence in vitro in order to study the mechanisms of senescence and its role in aging; the most common one being exposing cells to external DNA-damaging agents, such as for example UV radiation or chemical treatments. Senescence induced by DNA damage simulates extrinsic aging, since it is triggered by environmental factors. Replicative-Induced Senescence (RIS), on the other hand, is based on the fact that there is a limit on cell replication, called the Hayflick Limit, where cells stop all further division because of telomere attrition at each cell division [14]. Replicative-induced senescence, obtained by repeated subculturing, simulates intrinsic aging, since aging is a process inherently occurring in cells. This study therefore simulates replicative senescence by repeatadly subculturing fibroblasts.

3.2 Cellular senescence

Cells are constantly exposed to internal and external stresses that induce cellular damage. When the DNA repair mechanisms become deficient and genomic stability is at risk, cells choose one of several developmental paths, one being senescence. Cellular senescence is a mechanism that is built into our DNA as a safeguard against the alternative cell fates of malignant transformation or cell death [15].

Senescent cells have entered an irreversible state whereby they have ceased to divide. This permanent cell cycle arrest is accompanied by phenotypic alterations including metabolic reprogramming and pro-inflammatory secretome [16]. Although senescent cells can no longer replicate, they are alive and metabolically active. For example, cells enlarge even in the absence of cell division. Still, senescence is a paradoxical response, as it is propagated to neighbouring cells. Senescence is spread through secretion of so-called Senescence-Associated Secretory Phenotypes (SASPs) consisting mainly of pro-inflammatory extracellular modulators such as cytokines. These can induce or accelerate a state of chronic inflammation in nearby and distant cells and disrupt normal tissue function, which drives age-related diseases and alterations [2] [17].

Senescence is a highly heterogeneous phenomenon, exhibiting variations with regard to what induced the stress (replicative stress, UV radiation or chemical agents), its tissue and cellular context (fibroblasts, melanocytes, keratinocytes, epithelial tissue, connective tissue), and the diversity in the composition and abundance of the factors that are secreted (SASP), as well as the different pathologies and alterations that senescent cells have been linked to [18]. Understanding senescence heterogeneity requires further scrutiny when conducting anti-aging research. When investigating biomarkers for cellular senescence, this study therefore looks at three distinct and fundamental phenotypical alterations occuring during senescence; alterations in nuclear integrity, in cellular metabolism and in intercellular communication.

Literature on senescence has identified several candidate biomarkers of cellular senescence. The three categories of senescent biomarkers this study discusses are biomark-

ers of DNA damage (3.2.1), biomarkers of metabolic alterations (3.2.2) and SASPs (3.2.3), as per Figure 3.1.

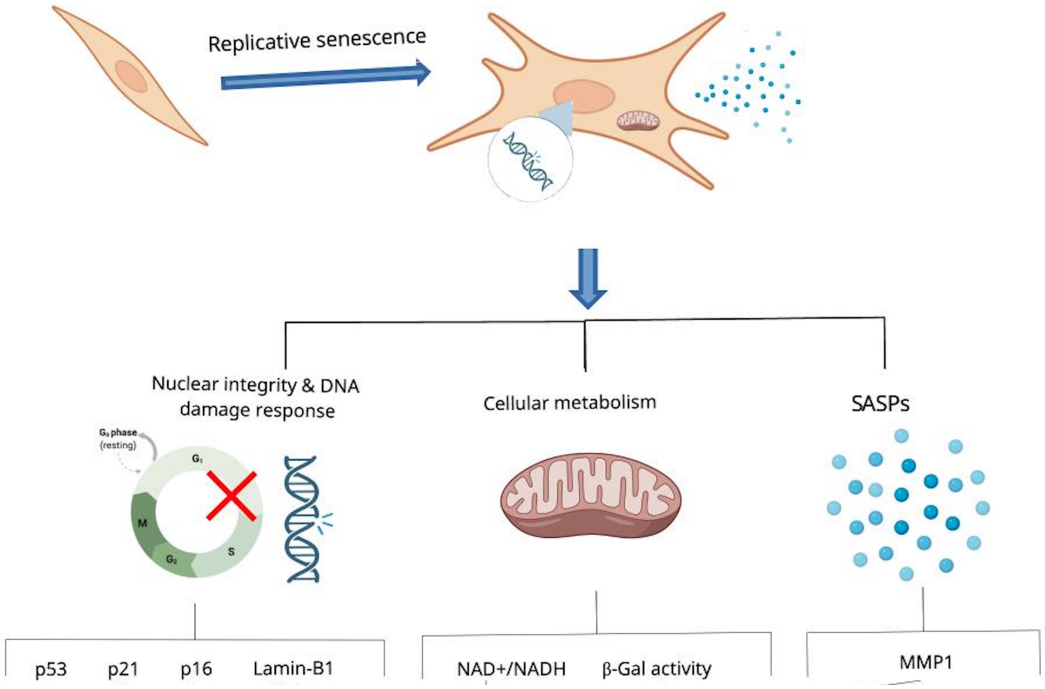

Figure 3.1: Senescence-associated features and their downstream targets.

3.2.1 Nuclear integrity and DNA Damage Response

A type of marker that has been linked to senescence are tumor-suppressors, such as p53, $p21^{WAF1}$ and $p16^{INK4a}$. The protein p53 is activated by damaged DNA and accumulates when a cell becomes stressed. It initiates the production of $p21^{WAF1}$, which in turn causes cell cycle arrest. A parallel mechanism to induce cell cycle arrest is the activation of p16, which inhibits cyclin-dependent kinases (CDKs) and stops the cell from proliferating [19].

Loss of Lamin-B1 also serves as a recognizable biomarker for senescence [20]. Lamin-B1, a major component of the nuclear lamina, contributes to maintaining nuclear structure. A downregulation of Lamin-B1 has been associated with an altered nuclear morphology and transcriptomic changes and has been implicated in senescence both in vitro and in vivo [21][22]. Studies have shown that senescence induced through replicative exhaustion in Human Dermal Fibroblasts involves decreased Lamin-B1 protein levels due to reduced transcription of the LMNB1 gene and inhibition of mRNA translation [22].

3.2.2 Cellular Metabolism

β-Galactosidase is a lysosomal enzyme that cleaves terminal β-Galactose residues. An increase in its activity level can cause the breakdown of macromolecular proteo-

glycans and damage to basement membranes [23], which is a metabolic change. Judith Campsini [24] discovered that β-Galactosidase activity is detectable in senescent cells at pH 6.0, serving as an indicator of cellular senescence. Senescence-Associated β-Gal is an enzyme responsible for cleaving terminal β-Galactose residues. At pH 6.0, the β-Gal activity is detectable for cells experiencing replicative senescence. Thus, it has become a well-established indicator of cellular senescence, as senescent cells typically exhibit increased SA-β-galactosidase activity compared to non-senescent cells [25].

NAD+ is one of the most abundant molecules in the body, essential for hundreds of enzymatic reactions. It acts as a redox-coenzyme involved in cellular metabolism by transitioning between its oxidized (NAD+) and reduced state (NADH). This fundamental role makes it essential for the functioning of all living cells [26]. Additionally, NAD+ serves as a substrate for NAD-consuming enzymes like Sirtuins and CD38. CD38, in particular, consumes NAD+ during the synthesis of cyclic ADP ribose, contributing to its depletion, which is accelerated in senescent cells, fostering a degenerative feedback loop between NAD+ loss and increased senescence [27]. Moreover, NAD+ levels have been observed to decline with age [28][29][30]. The NAD+/NADH ratio has emerged as a crucial biomarker for senescence, reflecting shifts in cellular metabolism and redox balance [3]. Mitochondrial dysfunction, often driving senescence, is characterized by a disrupted NAD+/NADH ratio. This disruption not only compromises cellular redox balance but also impairs NAD+ availability, subsequently hampering sirtuin activity. These disturbances play a pivotal role in regulating cell cycle arrest and modulating the senescence-associated secretory phenotype (SASP) which is independent of cellular growth arrest [31].

3.2.3 Senescence-Associated Secretory Phenotype (SASP)

A common category of senescent biomarkers are SASPs. Senescence influences the Extracellular Matrix (ECM) turnover, particularly through Matrix Metalloproteinases (MMPs). MMPs are a type of SASP factors that degrade ECM components. The degradation process of the ECM has been implicated in many age-related pathologies, such as premature aging syndromes, wrinkly skin, tumor progression etc [32]. Senescence-Associated (SA) Matrix Metalloproteinase-1 (MMP1) in particular plays a significant role in degrading Collagen type-I, -II and -III within the ECM [33].

3.3 Detection methods of senescence

Measuring cellular senescence is complex, and there is no single approach that is accepted. In previous studies, numerous techniques have been explored to identify and analyze this phenomenon. These methods vary with regard to principle, target, as well as with regard to what senescence-associated feature they capture. The following sections give an overview of the key senescence detection methods in the literature. Figure 3.2 is a complement to Figure 3.1 (senescence-associated features and their downstream targets), adding these detection methods of downstream

targets.

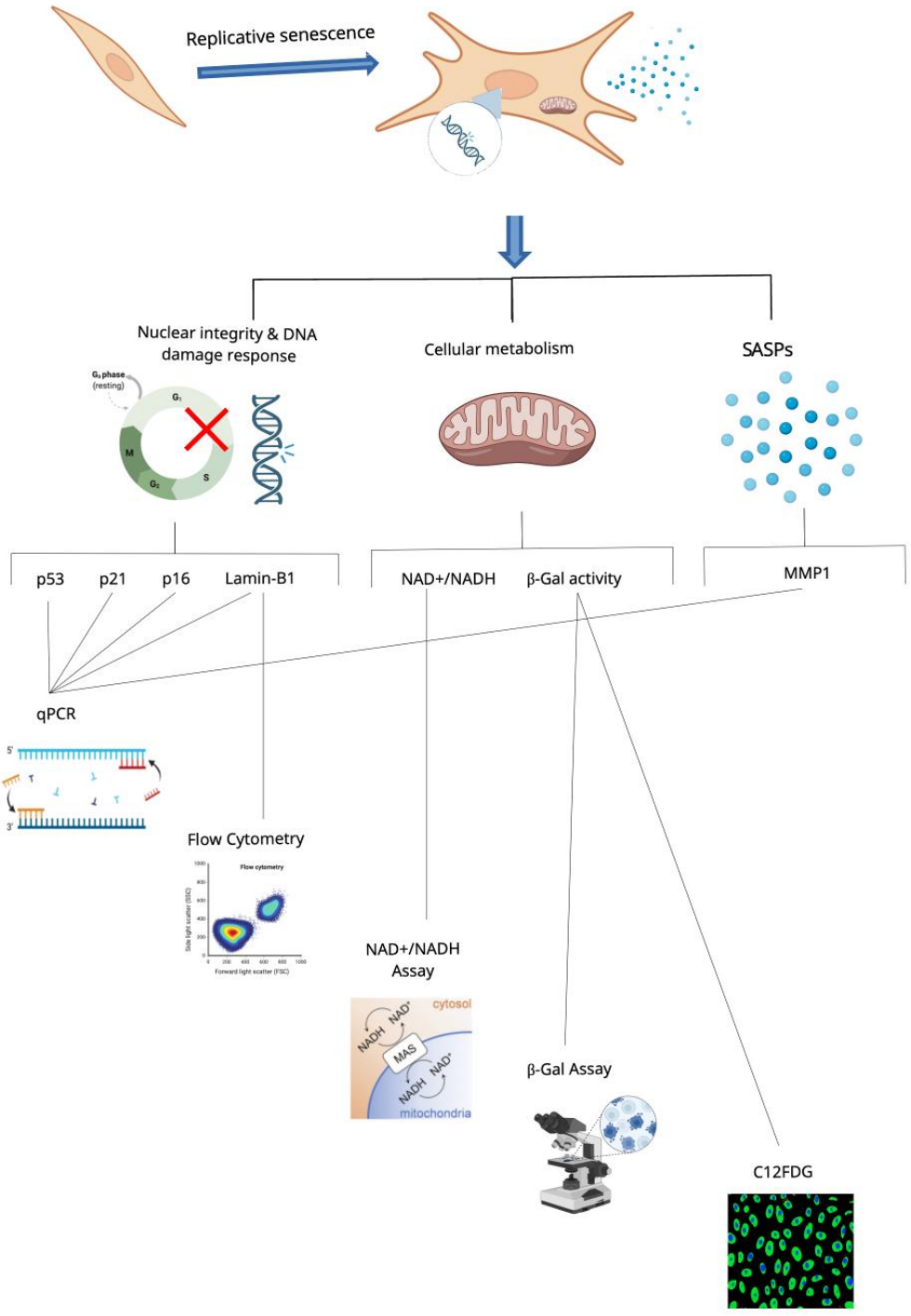

Figure 3.2: Detection methods of downstream targets.

3.3.1 NAD+/NADH-Glo Assay

The NAD+/NADH ratio has been commonly employed as a quantifiable marker for senescence in previous studies. In the literature, two main methods have been utilized for quantifying intracellular NAD+ and NADH. Yuan et al. [34], among others, have utilized colorimetric kits for quantification. This method relies on a NAD Cycling Enzyme Mix to act on NAD+/NADH, resulting in a color change that can be measured spectrophotometrically. Secondly, methods employing bioluminescence as a means for detection and quantification of NAD+/NADH are also commonly used. The amount of bioluminescence emitted from a sample correlates with the levels of NAD+ and NADH present. The NAD+/NADH ratio is subsequently calculated by dividing the bioluminescence value obtained from a NAD+ sample by the value obtained from its corresponding NADH well [35].

3.3.2 Quantitative Reverse Transcription-PCR (qPCR)

Quantitative Reverse Transcription-PCR (qPCR) measures the relative expression of genes in a sample. The primers stain DNA-segments correlating to specific genes. If DNA-segments are defect or become silent because of senescence, the senescence can then be measured by comparing the relative expression of that specific gene in young and old cells. Literature on metabolic pathway engineering found statistically significant differences in the expression level of p53, $p16^{INK4a}$, $p21^{WAF1}$ and Lamin-B1 in old and young cells, and therefore these are likely involved in senescence-related pathways [20].

3.3.3 Flow Cytometry

Flow cytometry is another technique for quantifying protein expression levels in cells and has emerged as a valuable technique for assessing cellular senescence. This method employs fluorescently labeled antibodies that specifically target proteins of interest, taken with care to select fluorophores with minimal spectral overlap. One of the key biomarkers analyzed using flow cytometry in the context of cellular senescence is Lamin-B1; the above-mentioned component of the nuclear lamina. In a study conducted by Freund et al. [20], flow cytometry was used to quantify the loss of Lamin-B1 in HDFs undergoing replicative senescence. The authors observed a significant decrease in Lamin-B1 levels in late-passage HDFs compared to their early-passage counterparts, further validating downregulation of Lamin-B1 as a reliable biomarker for cellular senescence.

3.3.4 SA-β-Galactosidase assay

SA-β-Galactosidase (β-Gal) activity serves as a widely recognized biomarker for cellular senescence. Senescence-associated (SA) β-Gal is β-Gal activity that can be measured at a pH level 6.0 in in-vitro cultures of cells that are senescent [36][37][25][13]. The β-Galactosidase staining has come to be the gold standard amongst methods for detection of senescent cells in vitro [38]. The principle of the assay is that cells

positive for β-Gal activity are indicated by blue staining. Thus, the proportion of stained (senescent) cells can be determined by manually counting the number of blue cells and dividing it by the total number of cells counted in a sample [36]. In pursuit of improved senescence analysis methods, the standard β-Gal assay is found to have significant limitations; it is time-consuming and lacks sensitivity.

3.3.5 C12FDG staining

As an alternative detection method of β-Gal activity, 5-dodecanoylaminofluorescein di-beta-D-galactopyranoside (C12FDG), a fluorescent substrate for β-Gal activity, has been introduced for quantifying senescent cells in a sample [39][36]. Unlike the manual counting required by the SA-β-Gal assay, C12FDG utilizes fluorescence, allowing imaging cytometers to quantify stained (i.e. senescent) cells in a more rapid and sensitive manner. Fluorescence-based C12FDG staining is particularly advantageous for high-throughput screening applications, enabling automated quantification of senescence levels across multiple treatment conditions or active ingredients [40].

3.4 Treatments to combat senescence

A further aim of this study is to investigate naturally-derived compounds as potential treatments for boosting the NAD+/NADH ratio. The literature indicates flavonoids (Quercetin, Apigenin, Kaempferol) as naturally-derived compounds able to boost this biomarker. Although 78c is a synthetic compound, the literature highlights its potency in boosting the NAD+/NADH ratio, making it a relevant candidate to include as a positive control of the treatments.

3.4.1 78c

It has been established that senescent cells upregulate the CD38 enzyme, which accelerates the depletion of NAD+ [41]. Inhibition of CD38 activity has emerged as a viable strategy to counteract NAD+ depletion and potentially ameliorating age-related senescence [42]. Compound 78 (78c) is a synthetic CD38-inhibitory chemical that has been proven to be a potent treatment for NAD+ associated decline [43]. Some in-vitro studies have even used 78c as a positive control for CD38 activity inhibition [44][45]. 78c is a senolytic drug; it acts by selectively eliminating senescent cells through a process called senolysis [46]. A study by Peclat et. al [47] found that treating naturally aged mice with the CD38 inhibitor 78c resulted in increased health- and lifespan.

3.4.2 Flavonoids

Flavonoids, a group of natural compounds found in plants, fruits, tea or wine have garnered attention for their potential to combat senescence [48]. These bioactive substances possess a wide range of beneficial health effects, including antioxidant [49][50], anti-inflammatory [51][52] and anti-carcinogenic properties [53], making

them an interesting candidate for pharmaceutical, medicinal and cosmetic applications [54].

Quercetin is a flavonoid that has been used as treatment for senescence [55][56]. Similarly to 78c, Quercetin is a senolytic agent that functions by inhibiting the CD38 NADase, thereby decreasing the degradation of NAD+. A key difference between them is that 78c is a synthetic chemical, while Quercetin can be found in nature. Quercetin has been shown to effectively treat senescent endothelial cells, as well as mouse bone marrow-derived mesenchymal stem cells [54]. Sohn E. et. al [57] studied treating aged HDFs with Quercetin and found that it directly reduced reactive oxygen species (ROS) levels, and alleviated mitochondrial dysfunction.

Another approach involves the use of senomorphic flavonoids, such as Apigenin and Kaempferol, which target senescence by eliminating the adverse effects of senescence without inducing cell death. Apigenin and Kaempferol have been proven to strongly suppress SASPs in vitro [58]. In a study by Thakurdesai et. al [59], Apigenin was even used as a positive control for inhibition of CD38.

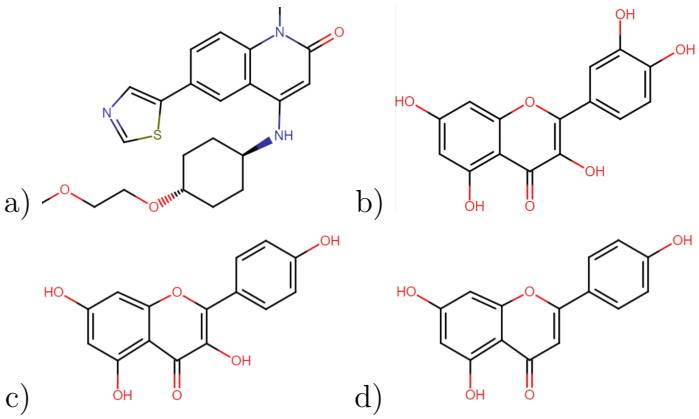

Figure 3.3: Chemical structures of a) 78c, b) Quercetin, c) Kaempferol and d) Apigenin.

4
Methods

4.1 Cell culturing and subculturing

Cell culturing and subculturing was performed according to the in-house protocol provided by Oriflame Cosmetics. HDFs were obtained from healthy donors, cultured in Biolite T75 culture flasks (Thermo Scientific Cat.#130190) and maintained in a 5% CO_2 incubator (Thermo Scientific, Heracell™150i) at 37℃. Cells were cultivated in Dulbecco's Modified Eagle Medium (DMEM) (Gibco Cat.#31966047) containing 10% Fetal Bovine Serum (FBS) (Gibco Cat.#26140079). Cell culture media was replaced once every three days until a confluency of approximately 80% was obtained. After obtaining the desired confluency the cells were either subcultured to a new culture flask or seeded to a culture plate.

Subculturing was performed by aspirating the media from the T75 flask, washing the flask with PBS -/- Mg_{2+} and Ca^{2+} (Gibco Cat.#14190-094) and adding 1.5ml TrypLE Express (Gibco Cat.#12604-013) before incubating it for 5 minutes or until the cells detach from the flask. Following incubation, 8.5ml Dulbecco's Modified Eagle Medium (DMEM) (Gibco Cat.#31966047) containing 10% Fetal Bovine Serum (FBS) (Gibco Cat.#26140079) and 1% Penicillin-Streptomycin (PEST) was added to the flask and mixed thoroughly to create a cell suspension. Lastly, the cell suspension and fresh media was added into a new culture flask or to a culture plate.

A senescence-associated phenotype in HDFs was induced by repeatedly subculturing the cells. After multiple cell divisions, the cells entered a state of replicative-induced senescence (RIS). Using microscopic imaging, the characteristic senescent morphology was confirmed by its increased cell size, flattened morphology and decreased proliferation rate [13].

4.2 Detection methods of senescence

Below is a detailed description of the protocols of the assays that are included in this study. They are based on established methods from literature and on general manufacturer's instructions. They were optimized and tailored for application to a replicative-induced senescence model using HDFs. Some of the protocols utilize proprietary reagents from commercially available kits, for which the specific chemical compositions are protected under patent and therefore not disclosed by the manufacturers.

4.2.1 NAD+/NADH Assay

To prepare the active treatments, the compounds 78c (Sigma, Cat.#5387630001), Quercetin (Sigma, Cat.#Q4951), Apigenin (Sigma, Cat.#10798) and Kaempferol (Sigma, Cat.#60010) were diluted in dimethyl sulfoxide (DMSO) (Fischer, Cat.#BP231) to create a stock solution of 20mM. The stock solution was further dissolved in Dulbecco's Modified Eagle Medium (DMEM) (Gibco, Cat.#10566016) containing 10% Fetal Bovine Serum (FBS) (Gibco, Cat.#26140079) and 1% Penicillin-Streptomycin (PEST) to the desired end concentration, before adding it to a plate according to the predetermined layout.

Treatment was initiated by aspirating cell culture media from the wells and replacing it with 100μL of a treatment solution. The plate was then incubated (Thermo Scientific Heracell™150i) under standard cell culture conditions (37°C, 5% CO_2) for the specified treatment duration (e.g. 24h). Afterwards, the treatment solution was aspirated and the wells washed with PBS. Lastly, 100μL of PBS was added to each well, and the NAD+/NADH-Glo™Assay as well as cell viability assessment were conducted. After incubation, the Luciferin Detection Reagent and the NAD+/NADH-Glo™Detection Reagent (Promega, Cat.#G9071)) were prepared according to the manufacturer's instructions. Media was removed from the cells, 50μL PBS -/- Mg_{2+} and Ca^{2+} (Gibco Cat.14190-094) was added to each well, as well as 50μL 1% Dodecyltrimethylammonium bromide (DTAB) (Sigma, Cat.#D8638). Next, 50μL of each well was transferred to NADH columns. 25μL 0.4M HCl was added to the remaining NAD+ columns. The plate was then incubated, firstly at 60°C without CO_2 for 15 minutes and subsequently at room temperature for 10 minutes. Thereafter, 25μL Trizma base (Sigma Cat.#T1503) was added to NAD+ columns, and 50μL HCl/Trizma was added to NADH columns. 50μL of all wells were transferred to a new 96-well cell culture plate, and 50μL of the prepared NAD+/NADH-Glo™Detection reagent was added to each well on the new plate. After a final incubation of 30-60 minutes, the bioluminescence was read using Cytation™3 Cell Imaging Reader (BioTek Instruments Inc.) with an integration time of 0.25–1 seconds per well.

The NAD+/NADH-ratio is not presented in the raw data of luminescence values. To be able to analyze the bioluminescence results from the Cytation™3 Cell Imaging Reader, the ratio is calculated by dividing the NAD+ with its NADH value. Statistical analyses comparing groups (e.g. untreated versus treated samples, or between samples in different passages) were calculated using GraphPad Prism software (GraphPad Software Inc., San Diego, CA, USA).

Cell viability was assessed on HDFs exposed to a treatment. The cell viability was measured using the CellTiter-Glo 2.0 Luminescent Cell Viability Assay (Promega, Cat.#G9241) according to the manufacturer's instructions. In brief, the ATP content was measured by adding CellTiter-Glo®Reagent in a volume equal to that of the media, followed by a 10-minute incubation before reading bioluminescence using Cytation™3 Cell Imaging Reader (BioTek Instruments Inc.). Using the resulting bioluminescence values, the viability percentage compared to untreated was

calculated.

4.2.2 Quantitative Reverse Transcription-PCR (qPCR)

During RNA extraction, the total cellular RNA was isolated using the RNeasy mini kit (Qiagen Cat.#74106) according to the manufacturer's instructions. The total RNA was reverse transcribed into cDNA using the iScript Advanced cDNA Synthesis kit (Bio-rad, Cat.#172-5038), also as per the manufacturer's instructions, followed by a 20-minute incubation in a qPCR CFX96 Real Time System (Bio-rad) at 46°C for reverse transcription and subsequently for 1 min at 95°C for RT inactivation. Lastly, qPCR reactions were performed using Sso Advanced SYBR Green®(Bio-rad, Cat.#172-5274) as well as gene-specific forward and reverse primers. Target gene expressions were normalized against GAPDH (Glyceraldehyde 3-Phosphate Dehydrogenase), the housekeeping gene. Reactions were run in the qPCR CFX96 Real time System (Bio-rad) with a thermal cycling program: 95°C for 3 minutes as initial denaturation, 39 cycles of 10 seconds at 95°C for denaturation and 30 seconds at 60°C for annealing. Gene expression analysis was performed using BIO-RAD CFX Maestro Software together with the comparative $\Delta\Delta$Ct methodology, given a stable expression of the reference gene. Statistical analyses were performed on the resulting ΔCt values. Every experiment comprised two biological replicates as well as two technical replicates for each sample. Technical replicates exhibiting variations greater than 20% were excluded from further analysis to ensure data integrity.

4.2.3 Flow Cytometry

After a 48-hour incubation period, cells seeded on a 12-well plate were detached by using 200μL of TrypLE Express (Gibco Cat.12604-013). The wells were washed with 500μL of PBS, and the cell samples were collected and centrifuged. Following centrifugation, the supernatant was removed, the cell pellets resuspended in 100μL of PBS and 100μL of Fixation Buffer. A 1-hour incubation at room temperature allowed for fixation. Upon completion of the fixation step, 700μL Staining Solution was added to each sample, and the samples were centrifuged again. The supernatant was discarded, and the pellets were resuspended in 500μL Staining Buffer. After another round of centrifugation and supernatant removal, the cells were stained with varying concentrations of antibodies for 1 hour at room temperature. Specifically, Lamin-B1 antibodies were diluted to the appropriate concentration in perm buffer, and 50μL of the diluted antibody solution was added to the respective samples. Following the 1-hour antibody staining, the samples were washed once with 1mL Staining Buffer, before staining samples for Lamin-B1 with secondary antibodies 100X 1:100 in 50μl permeabilization buffer for 1 hour at room temperature. Finally, the cells were filtered through a cell strainer into 5mL round-bottomed flow tubes and vortexed to ensure a homogeneous suspension, before proceeding with flow cytometry analysis (ACEA NovoCyte 2000R). The flow cytometry analysis was performed with stop conditions set at either 100μL or 12,000 events on the P2 gate, and a forward scatter (FSC-H) threshold greater than 100,000 was applied to exclude

debris and ensure accurate detection of cellular events.

4.2.4 SA-β-Galactosidase assay

The Senescence-Associated β-Galactosidase activity was measured by using the Senescence Detection kit (Abcam, Cat.#ab65351) according to manufacturer's instructions. For a 12-well cell culture plate, media was removed and washed once with 1ml PBS. Then, 0.5mL Fixative Solution (included in the kit) was added and the cells were incubated for 10-15 minutes at room temperature and subsequently washed twice with PBS. Per well, the Fixative solution contained 470μL Staining Solution, 5μL Staining Supplement and 25μL X-Gal. Lastly, after adding 0.5mL Staining Solution Mix per well, the plate was covered and incubated (Thermo Scientific Cat.#130190) at 37°C (no CO_2) for 24 hours. After incubation, the cells were washed twice with PBS before observation under a converted color microscope. Pictures were taken with a 20x objective with corresponding phase contrast (Ph) for cell counting. Approximately 10-12 pictures were taken per well to reach a cell count of more than 400 cells. Finally, cells were counted using ImageJ software to calculate the percentage of stained cells, by dividing the number of blue-stained cells with the total amount of cells counted.

4.2.5 C12FDG staining

Cells were seeded on a MicroWell 96-Well Optical-Bottom Plate (Thermo Scientific, Cat.#165305), which are optimized for fluorescence in cell culture and microscopic applications. For adherent fibroblast cells, the culture media was removed, and the cells were washed twice with PBS. Next, the cells were fixated using the Fixative Solution from the Senescence Detection kit (Abcam, Cat.#ab65351) for 10-15 minutes at room temperature. The cells were then washed twice with PBS. The C12FDG solution was prepared by diluting it 100X in PBS and added to designated wells. The plate was then covered to protect it from light and incubated for 10 minutes at 37°C (no CO_2) for 1 hour. It was washed with PBS and lastly, 100μL PBS was added. To label the fixed cells, DAPI (4',6-Diamidino-2-Phenylindole, Dihydrochloride) (Thermo Scientific, Cat.#D1306) was diluted 100x in PBS and added to designated wells, followed by a five-minute incubation. The cells were washed once with PBS, and then PBS was added again, before imaging the cells using Cytation™3 Cell Imaging Reader (BioTek Instruments Inc.).

4.3 Statistical analysis

Statistical analyses were based on data from experiments on three or more independent donors, to ensure reliability and reproducibility of the findings. Unpaired Student's t-test was used to determine the statistical significance of the results. A significance threshold was set to $p \leq 0.05$ for a test to be considered statistically significant. In the results, * indicates $p \leq 0.05$, ** indicates $p \leq 0.01$, *** indicates $p \leq 0.001$, **** indicates $p \leq 0.0001$, and ns indicates a non-significant difference.

5

Results and Discussion

5.1 Candidates for the in-vitro cell-based model

This study aimed to develop an in-vitro cell-based model for objective quantification of replicative-induced senescence in HDFs. The results show that several of the established methods that were assessed are suitable candidates to be included in the proposed model.

5.1.1 NAD+/NADH assay

The NAD+/NADH-Glo™assay measured a statistically significant difference between old (high passage) and young (low passage) cells, with regard to the relative emitted bioluminescence, corresponding to the NAD+/NADH ratio (as seen in figure 5.1). This result was consistent across all experiments, which included three independent cell donors with varying passage numbers. This is in accordance with previous studies and validates the NAD+/NADH-Glo™assay for this particular cell model [28][29][30].

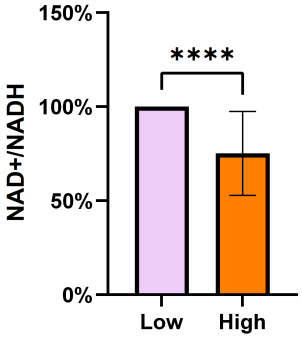

Figure 5.1: Average NAD+/NADH ratio between HDFs in low and high passage of three independent donors.

The difference in bioluminescence between biological replicates was small and insignificant. Consequently, the assay was not particularly volume sensitive. Therefore, calculating the standard deviation to assess intra-assay variability was deemed superfluous. Regarding the inter-assay variability, the variation in replicative lifespan between donors was substantial. There was no clear, consistent relationship

between donor age and the replicative lifespan of fibroblasts in culture. This is in line with evidence in literature, proving that there is only a small or insignificant inverse correlation between donor age and fibroblast proliferative potential [60]. In other words, the replicative lifespan varies widely even among cell lines from donors of similar sex and age. As the passage number at which senescence was reached varied significantly between donors, cells were passaged until they exhibited a senescent morphology and categorized as "low" or "high" passage, rather than being named by their specific passage number.

5.1.2 Quantitative Reverse Transcription-PCR (qPCR)

Figure 5.2 presents the average fold change in gene expression for TP53 (p53), CDKN1A (p21), CDKN2A (p16), MMP1 and LMNB1 (Lamin-B1) in low-passage (5-12) and high-passage (20-34) HDFs.

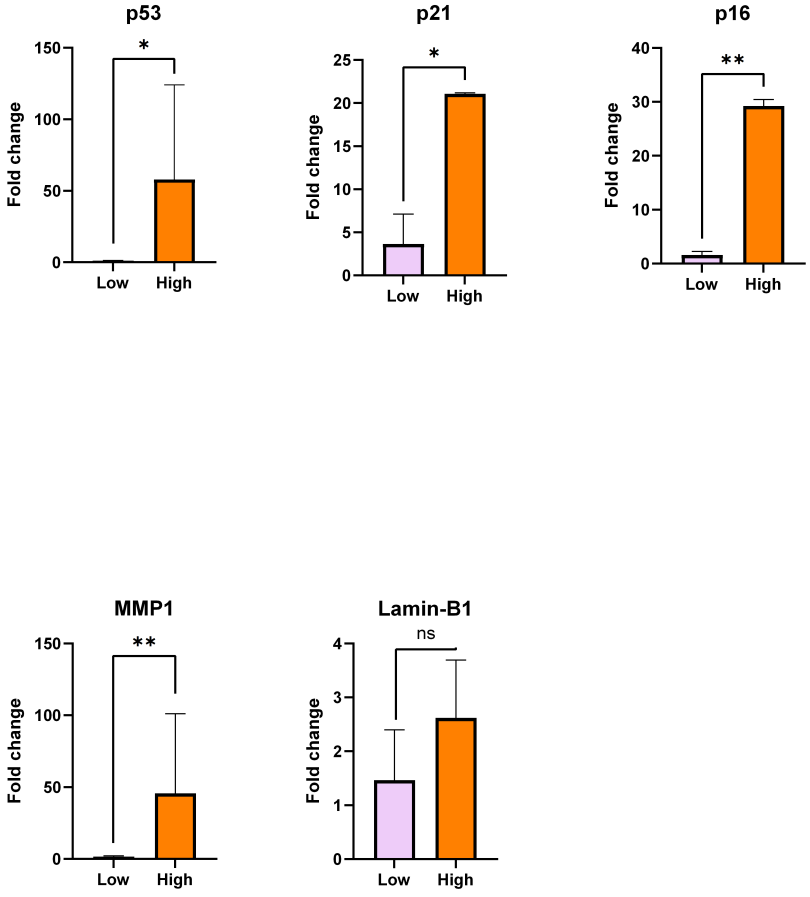

Figure 5.2: Average fold change comparing cells in low and high passage for proteins p53, p21, p16, MMP1 and Lamin-B1, (n=3).

The qPCR analysis revealed that several genes involved in DNA damage and cell cycle arrest pathways were upregulated following replicative-induced senescence in three independent HDF donors (n=3), including TP53 (p53), CDKN1A (p21) and CDKN2A (p16). Moreover, the expression of MMP1, which is associated with the Senescence-Associated Secretory Phenotype (SASP), also exhibited a trending upregulation, indicating an increased secretion of pro-inflammatory and ECM-degrading factors in senescent cells. These findings align with the existing literature on the transcriptional changes that have been observed during cellular senescence [19][61][62].[33]

Unexpectedly, the expression of LMNB1, encoding the nuclear envelope protein Lamin-B1, was not downregulated in high-passage HDFs, as described in the literature [20]. In conclusion, most of the genes associated with senescence exhibited an expected upregulation. The observed expression pattern of the nuclear envelope protein Lamin-B1 deviated from what has been previously reported in the literature, highlighting the variability in the expression of biomarkers across different experimental setups.

5.1.3 Flow cytometry

Flow cytometry data are presented as data points on graphs. Figure 5.3 shows dot plots illustrating the cell population in low-passage cells (p.11). Figure 5.3a shows live cells as P1, while figure 5.3b shows singlets as P2 from the live population P1.

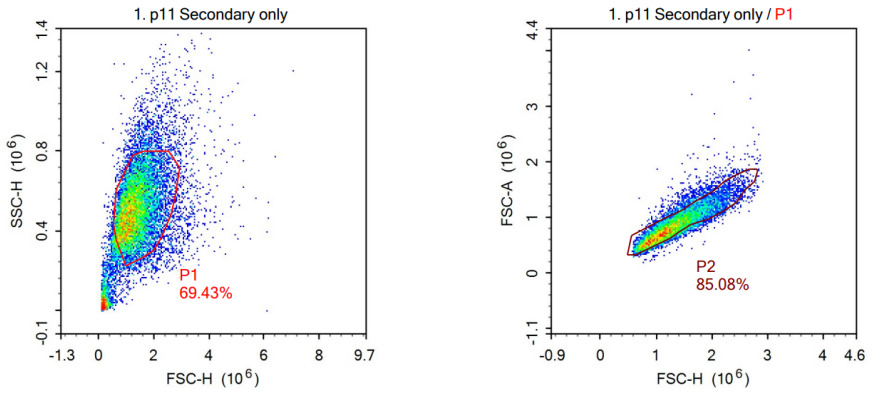

Gate	Count	% All	Median X	Median Y
All	14,308	100.00%	1,231,857	470,121
P1	9,934	69.43%	1,298,444	495,374

Gate	Count	% P1	Median X	Median Y
P1	9,934	100.00%	1,298,444	855,701
P2	8,452	85.08%	1,245,173	816,724

Figure 5.3: Dot plot of the cell population displaying (a) SSC-H vs FSC-H and (b) singlets in FSC-A vs FSC-H for the Lamin-B1 stained sample with cells in passage 11.

Each dot represents an individual cell analyzed by the flow cytometer. Forward scatter (FSC) on the x-axis measures cell size, while side scatter (SSC) on the y-axis measures cell complexity. These dot plots enable differentiating cell populations by size and granularity. Gating defines regions to isolate specific populations and can be seen as the manually drawn red lasso-line separating live/dead cells in Figure 5.3a.

Figure 5.4 shows histograms representing the distribution of the detected fluorescence intensity for the Lamin-B1 antibody compared to the unstained secondary sample. The Lamin-B1 antibody showed sufficient staining in the cells, with a clear separation of the histogram for Lamin-B1 from the sample stained only with the secondary antibody.

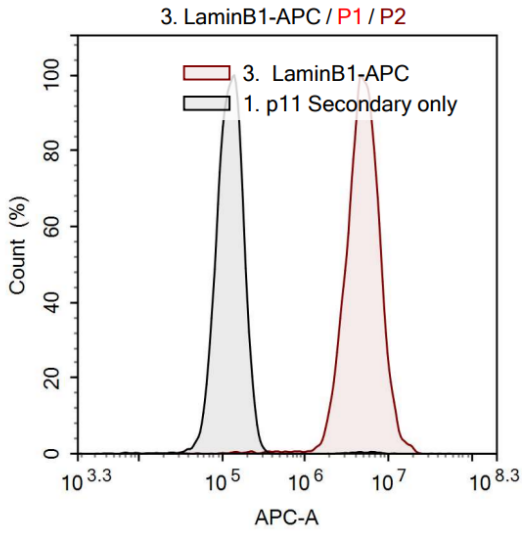

#	Sample	Gate	Count	% P2	Median X
1	3. LaminB1-APC	P2	7,995	100.00%	5,083,364
2	1. p11 Secondary	P2*	8,452	100.00%	128,890

Figure 5.4: Histograms of samples from low-passage HDFs (p.11) stained with Lamin-B1 compared to sample only stained with secondary antibody.

Figure 5.5a shows the final histograms for low-passage (p.11) HDFs stained only with a secondary antibody, low-passage HDFs stained for Lamin-B1 (blue), and high-passage HDF stained for Lamin-B1 (red). In figure 5.5a, a negative shift can be seen from the low-passage to the high-passage cells along the x-axis. This translates into a lower expression of the Lamin-B1 protein in cells in passage 34 (high) compared to cells in passage 11 (low). This finding aligns with the previous studies, claiming a downregulation in high-passage compared to low-passage HDFs as a marker for senescence. This finding is also presented in a bar chart, seen in figure 5.5b.

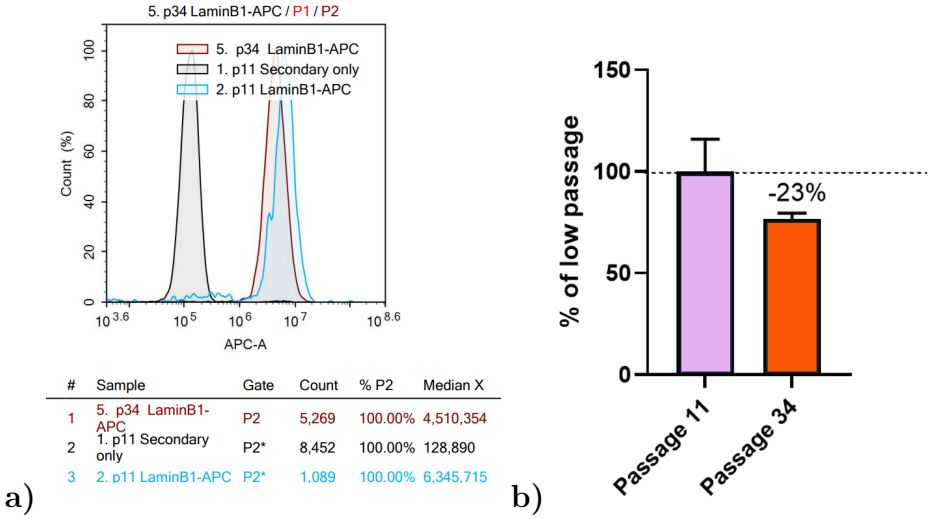

Figure 5.5: Lamin-B1 concentration in low- and high-passage HDFs. (a) Histograms of samples in passage 11 and passage 34 stained with Lamin-B1 compared to sample only stained with secondary antibody. (b) Bar chart of Lamin-B1 protein expression for passage 11 and passage 34, (n=1). Samples are compared to passage 11 which was set to 100%. Values displayed are mean (SD) of technical replicates.

The flow cytometry data revealed a downregulation of the Lamin-B1 protein concentration during senescence, consistent with literature reports. This contrasts with the resulting expression patterns obtained from the qPCR experiments. One possible explanation for this finding could be that Lamin-B1 is upregulated on a gene expression level to compensate for the loss of protein, or that the cell is not efficient enough to translate the RNA into protein [63]. Another plausible explanation for the discrepancy between LMNB1 gene expression and Lamin-B1 protein levels could be post-translational modifications, causing them to degrade before they can be used. However, it should be noted that these results are based on data from one donor (n=1). Thus, further experiments using other independent donors are warranted to validate this finding.

5.1.4 SA-β-Gal assay

The SA-β-Gal assay successfully stained senescent cells across three independent HDF donors (n=3). As expected, SA-β-Gal activity increased after exposing the cells to replicative stress. Figure 5.6a displays representative images of samples characterized by a low and high degree of senescence, as evidenced by the β-Gal staining. Figure 5.6b illustrates the statistical difference in SA-β-Gal activity between low and high-passage cells. The percentage of SA-β-Gal positive cells demonstrates a significant increase in the proportion of senescent cells in higher-passage fibroblasts compared to lower-passage cells. The average percentage of low-passage cells (passages 5-8) across all three donors was 15%$\pm$7.3. In contrast, the average percentage of old cells (passages 20-36) was 44%$\pm$18.1.

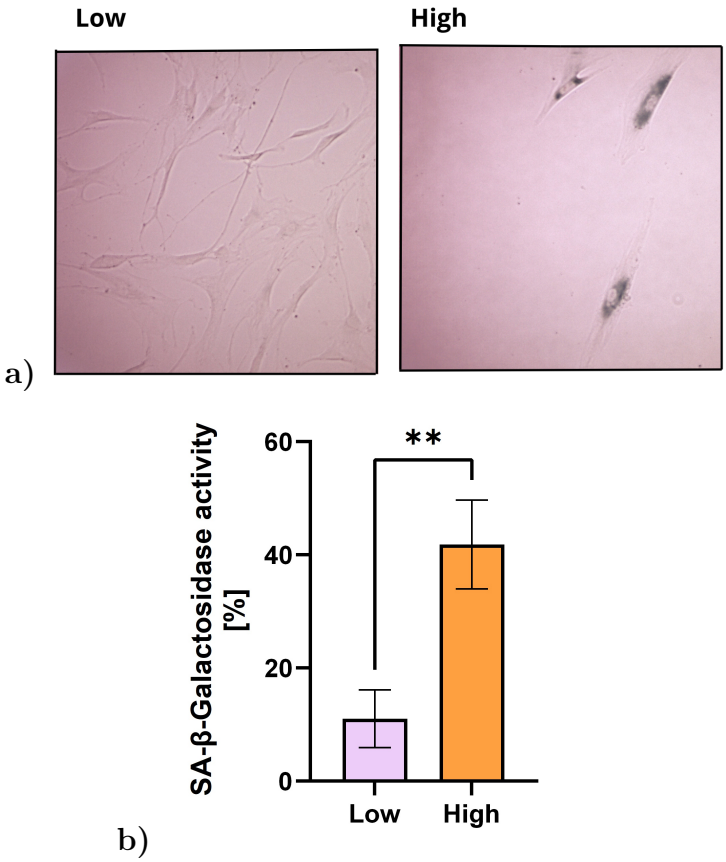

Figure 5.6: β-Galactosidase staining at pH 6.0. (a) Microscopic images of cells in high and low passage after staining for SA-β-Gal activity. (b) Plot of the average SA-β-Gal for three HDF donors (n=3), comparing low (5-8) and high (20-36) passage cells.

Examination of the microscopic images revealed that the SA-β-Gal-stained cells displayed a flattened and enlarged morphology, consistent with the characteristic features of senescent cells described in the literature [13]. This visual confirmation further validated the use of the SA-β-Gal assay to reliably detect and quantify the senescent cell population across different fibroblast donors. The observed morphological changes in the stained cells aligned with the expected senescent phenotype, providing a comprehensive assessment of cellular senescence in this in-vitro model.

The quantitative analysis demonstrated a significant increase in the percentage of SA-β-Gal-positive cells in higher-passage fibroblasts compared to its lower-passage counterpart. This indicates an accumulation of senescent cells, confirming that replicative stress is a driver of cellular senescence. While the percentage values varied substantially across the donors, as indicated by the relatively high standard deviation, the trend of older cells obtaining a higher staining percentage was statistically significant within each donor. Further details on each individual SA-β-Gal experiment can be found in Table A.1 in the appendix.

5.1.5 C12FDG staining

Figure 5.7 shows C12FDG-staining captured by fluorescence microscopy and is indicative of replicative-induced senescence by the larger cell population amongst low-passage cells compared to high-passage cells. High-passage cells that were positively stained with C12FDG displayed a stretched-out cell morphology characteristic of senescent cells [13].

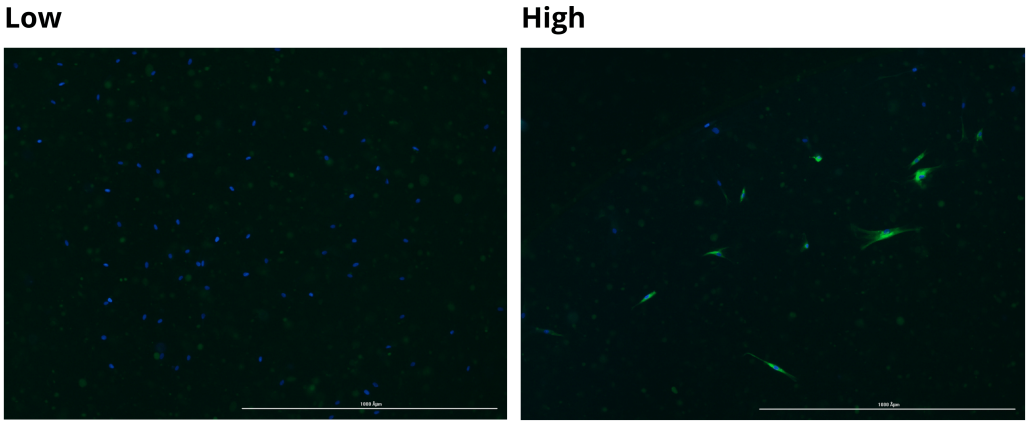

Figure 5.7: Fluorescent microscopic pictures with a 20x objective of C12FDG-stained cells in passage 11 (low) and passage 36 (high). DAPI-stained cells are shown as blue, C12FDG-stained cells are shown as green.

Interestingly, the green-stained cells in higher passage had an enlarged cell body compared to the lower-passage cells. This observation is consistent with previous analyses of the SA-β-Gal stained cells, where the typical senescent-cell morphology was displayed in the high-passage cells [13]. The consistent observation of enlarged cell morphology in high-passage cells provides further evidence of the senescent phenotype in this cell model. An issue that arose when conducting the C12FDG assay was the presence of significant background fluorescence, which disrupted the fluorescent microscopic pictures. Also, the assay encountered consistent corner effects: the cell density in the corner regions of the imaging well was higher compared to its center. While the Cytation 3 imaging system has the capability to count the number of cells in a well, automatic cell counting at the corners of a well may be unreliable.

In addition, the C12FDG assay employed automated measurements to determine the average cell population (via DAPI detection) and the total intensity per well (via C12FDG detection), on the basis of which a green fluorescence per cell ratio was calculated. As displayed in Table 5.1, the average green fluorescence ratio per cell was higher for high-passage (p.35) cells compared to low-passage (p.13) cells. All

individual sample data used to calculate these values can be found in the appendix table A.2.

Table 5.1: Average cell population, intensity and green fluorescence ratio per cell for cells in low and high passage

	Low	**High**
Population	9.82×10^{2}	1.22×10^{2}
Intensity [A.F.U]	5.96×10^{7}	2.62×10^{7}
Ratio [A.F.U/cell]	6.027×10^{1}	2.014×10^{2}

Higher green fluorescence ratio per cell was observed in the high-passage cell samples. The relative fluorescence intensity is expected to increase with a higher percentage of senescent cells in a sample. This finding is in accordance with the literature claiming that the C12FDG staining effectively detected the increased senescence-associated β-galactosidase activity in the high-passage cell population [39][36]. The automated measurement approach allowed for a quantitative assessment of the senescent phenotype, with the higher green fluorescence per cell ratio in the high-passage cells providing evidence of replicative-induced senescence in these cultures.

5.2 Efficacy of treatments

A further aim of this study was to measure the effects of flavonoid treatments on the senescent phenotype, using the NAD+/NADH assay as an acknowledged biomarker of senescence. The results were able to prove the efficacy of one of the flavonoids, Apigenin.

5.2.1 78c

After investigating the effect on HDFs of different concentrations (10nM to 200μM) of 78c for varying treatment times (1 hour up to 72 hours), no positive shift in the NAD+/NADH ratio was detected. Figure 5.8a illustrates the NAD+/NADH ratio for low- and high-passage HDFs as untreated (UT) and after treatment with 20μM 78c for 24h. The cell viability was compromised in high-passage HDFs when the treatment concentration used became too high or when the treatment time exceeded 24h. Figure 5.8b illustrates HDF cell viability percentages of untreated (UT) and after treatment with 20μM 78c, comparing high and low passage.

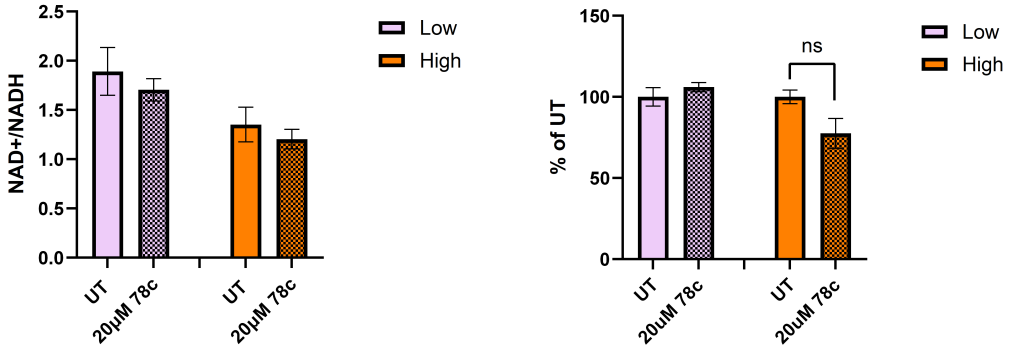

a) b)

Figure 5.8: 78c treatment on low- (p.10) and high-passage (p.22) HDFs. Untreated (UT) HDFs compared to treatment with 20μM 78c for a duration of 72h. (a) NAD+/NADH ratio. (b) Cell viability assessment.

Contrary to expectations, the CD38-inhibitor 78c did not boost the NAD+/NADH ratio. The literature claims that 78c can be used as a positive control for increasing NAD+ levels [44][45]. However, this does not align with the results in this study. One possible explanation is that differences in cell type and conditions may account for the divergent findings. The replicative-induced senescent HDFs used in this study may not be as responsive to 78c as the cell models in previous studies [43][44][45][47].

5.2.2 Quercetin

Figure 5.9a illustrates the NAD+/NADH ratio from one of the experiments, demonstrating the lack of a positive shift in this parameter. Figure 5.9b presents the results from a cell viability assay performed on the HDFs from the same experiment.

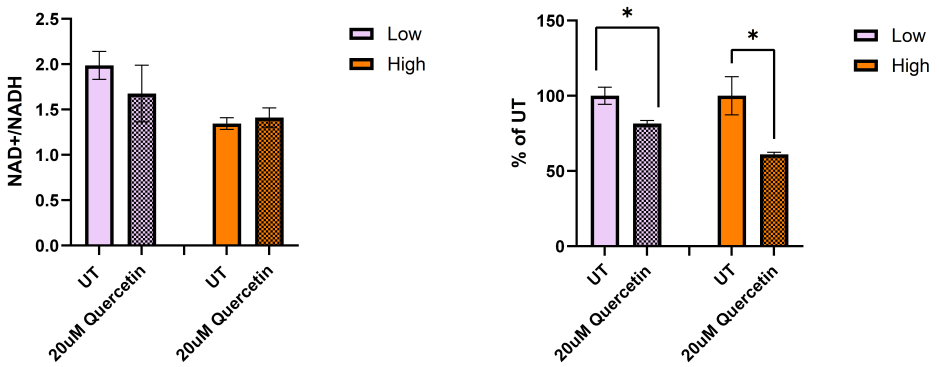

a) b)

Figure 5.9: Quercetin treatment on low- and high-passage HDFs. The HDFs were either untreated (UT) or treated with 20μM Quercetin for a duration of 24h. (a) NAD+/NADH ratio. (b) Cell viability assessment, including a DMSO control.

Treatment with 5-20μM Quercetin for 24 hours did not lead to a significant increase in the NAD+/NADH ratio either. The viability assay revealed that Quercetin was poorly tolerated by cells in both high and low passage, suggesting a potential cytotoxic effect at the concentrations tested. Student's t-test comparing UT and 20μM Quercetin revealed a statistically significant difference (*) between them, both in low-passage and high-passage cells.

In conclusion, neither of the two CD38-inhibiting treatments, 78c nor Quercetin, led to a statistically significant increase in the NAD+/NADH ratio in the replicative-induced senescent HDF model used in this study. The viability assay highlighted the limitations of these treatments, particularly in high-passage cells and for Quercetin even in low passage cells. Despite promising results in other studies [43][47], the efficacy of 78c and Quercetin cannot be assumed to translate directly into all cell models and experimental settings.

This may be because these are senolytic compounds, which function by selectively killing off senescent cells rather than modulating the senescent phenotype [64]. The severe compromise in cell viability observed after treating the HDFs with 78c and Quercetin, even at concentrations used previously on melanocytes [65], could be explained by the fact that fibroblasts may be less resistant to replicative stress compared to other cell types. This is further supported by the fact that dermal fibroblasts are located in the dermis, whereas melanocytes are situated in the outer epidermis, where they are subjected to chronic environmental stressors such as UV radiation [66].

5.2.3 Kaempferol

Treating low- and high-passage HDFs with Kaempferol at concentrations 0.1μM, 1μM and 10μM for a duration of 24 hours did not significantly increase the NAD+/NADH ratio, as shown in Figure 5.10a. Figure 5.10b illustrates how the cell viability of the HDFs increases following Kaempferol treatments in a dose-dependent manner.

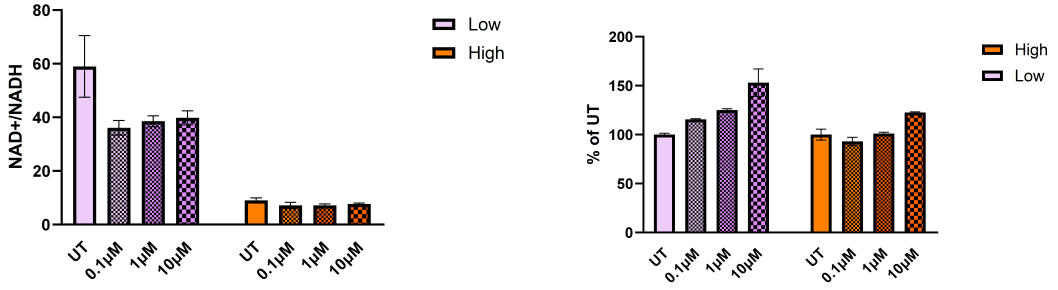

a) b)

Figure 5.10: Kaempferol treatment on low- and high-passage HDFs. The HDFs were either untreated (UT) or treated with 20μM Kaempferol for a duration of 24h. (a) NAD+/NADH ratio. (b) Cell viability assessment.

While Kaempferol did not significantly increase the NAD+/NADH ratio in this cell model and experimental setup, it likely exerted protective effects on the cells through other mechanisms, hence the dose-dependent increase in cell viability observed. This finding aligns with previous studies demonstrating the antioxidant effects of Kaempferol in HDFs, suggesting that its ability to mitigate oxidative stress and reduce reactive oxygen species levels could contribute to the observed increase in cell viability [67][68].

5.2.4 Apigenin

Treating HDFs in passage 12 and 35 with Apigenin at concentrations 0.1μM and 1μM for a duration of 24 hours significantly increased the NAD+/NADH ratio, as shown in figure 5.11. Statistical analysis using Student's unpaired t-test resulted in a p-value of 0.0042 (**) when comparing untreated with 0.1μM Apigenin treatment, and a p-value of 0.0336 (*) when comparing untreated with 1μM Apigenin treatment.

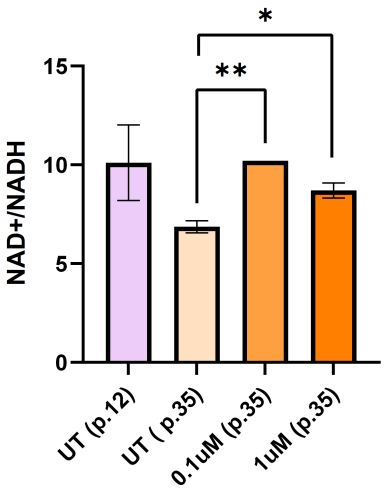

Figure 5.11: NAD+/NADH ratio after exposing HDFs in passage 12 (Low) and in passage 35 (high) to Apigenin treatment (0.1, 1, 10μM) for a duration of 24h.

The treatment with Apigenin boosted the NAD+/NADH ratio without inducing significant cytotoxicity. The senomorphic properties of Apigenin may explain its efficacy. Senomorphic compounds function by modulating the senescent phenotype as cells enter senescence, rather than selectively killing off senescent cells. Unlike the senolytic compounds, 78c and Quercetin, which compromised cell viability, Apigenin was able to positively influence the NAD+ redox state without negatively impacting the HDFs. Apigenin seems to be a suitable candidate for interventions aimed at boosting NAD+ in this cellular model. Further research into Apigenin's mechanisms in other models are needed to further explore its therapeutic potential.

6
Conclusion

To further understand the underlying mechanisms of skin aging, this study has looked at cellular senescence, with special emphasis on replicative-induced senescence in Human Dermal Fibroblasts. The aim was to develop an extensive model based on established quantifying methods to assess if they can be validated and contribute to objectively identifying and measuring senescent cells in the HDF cellular model. The following acknowledged methods for detecting biomarkers of senescence were employed: NAD+/NADH-Glo™assay kit, RNA Extraction and Quantitative Real-Time PCR (qPCR), Flow Cytometry, SA-β-Galactosidase assay and C12FDG staining.

The various assays employed in this study were able to quantify and detect replicative-induced senescence in Human Dermal Fibroblasts with varying degrees of success. NAD+/NADH-Glo™assay demonstrated a statistically significant decline in the NAD+/NADH ratio between low and high-passage HDFs. qPCR proved a significant upregulation of senescence-regulated genes like p53, p21, p16, and MMP1. Flow Cytometry measured an expected decrease in protein concentration of Lamin-B1 in old cells. SA-β-Galactosidase proved a higher percentage of β-Gal positive cells among high-passage HDFs and distinct morphological changes. When staining with C12FDG, the ratio of measured fluorescence per cell increased in higher-passage cells and it confirmed the characteristic senescent cell morphology. In summary, while the NAD+/NADH assay, Flow Cytometry, SA-β-Gal assay and C12FDG staining clearly distinguished senescent from non-senescent cells. However, the qPCR data for the Lamin-B1 gene expression was less conclusive. This highlights that not all assays worked exactly as intended for quantifying the specific senescence phenotypes in this cell model. Nonetheless, the combined data from multiple complementary techniques provided evidence that the main aim of establishing a robust in-vitro model of replicative senescence was largely fulfilled. However, it is important to note that the sample sizes in some assays were relatively small, warranting further validation with larger sample sets.

The model that is proposed in this study is based on these methods and is a good starting point to objectively quantify cellular senescence in HDFs in skin-aging research. The multi-method approach of combining several methods within a model enabled a comprehensive evaluation of various senescence markers and pathways, thus advancing our understanding of this complex phenotype. This has important implications for skin aging research by establishing a robust platform to study senescence mechanisms and test potential interventions. However, at this stage the model

does not describe the senescent phenotype in its full complexity; more biomarkers need to be taken into account. Research is ongoing and further research is needed to expand the tools in the toolbox.

A further aim of the study was to apply the NAD+/NADH-Glo™assay of the model, to test the effects certain flavonoid treatments (Quercetin, Apigenin and Kaempferol) have on skin senescence modulation, as compared to the chemical 78c treatment proven to reverse age-associated metabolic decline. Neither the flavonoid treatments Quercetin and Kaempferol, nor 78c caused any significant boost in NAD+/NADH ratio. On the contrary, 78c and Quercetin compromised cell viability at high concentrations or after long treatment exposure. Only treatment with low concentrations of Apigenin successfully increased the NAD+/NADH ratio in high-passage cells. However, further research is needed to confirm the results of the limited sample size in this study and to draw any steadfast conclusions.

While valuable insights were gained, further work is still needed to elucidate the heterogeneity and context-dependent nature of cellular senescence across different experimental conditions and cell types. Nonetheless, this research highlights the value of integrating multiple techniques to capture the multidimensional aspects of senescence biology.

Bibliography

[1] Chaudhary M, Khan A, Gupta M. Skin Ageing: Pathophysiology and Current Market Treatment Approaches. Current aging science. 2020;13(1):22-30.

[2] Shoubing Zhang ED. Fighting against Skin Aging. Cell Transplantation. 2018 4;27(5).

[3] López-Otín C, Blasco MA, Partridge L, Serrano M, Kroemer G. Hallmarks of aging: An expanding universe. Cell. 2023 1;186(2):243-78.

[4] Childs BG, Durik M, Baker DJ, van Deursen JM. Cellular senescence in aging and age-related disease: from mechanisms to therapy. Nature Medicine. 2015 12;21(12):1424-35.

[5] Muñoz-Espín D, Serrano M. Cellular senescence: from physiology to pathology. Nature Reviews Molecular Cell Biology. 2014 7;15(7):482-96.

[6] Yousefzadeh M, Henpita C, Vyas R, Soto-Palma C, Robbins P, Niedernhofer L. DNA damage-how and why we age? eLife. 2021 1;10.

[7] Gorbunova V, Seluanov A, Mao Z, Hine C. Changes in DNA repair during aging. Nucleic acids research. 2007;35(22):7466-74.

[8] Gorgoulis V, Adams PD, Alimonti A, Bennett DC, Bischof O, Bishop C, et al. Cellular Senescence: Defining a Path Forward. Cell. 2019 10;179(4):813-27.

[9] Joel John. Global Anti Aging Cosmetics Market Size Is Anticipated to Expand at a CAGR of 8% to Reach US$ 120 Billion By 2030 | Custom Market Insights Study; 2023.

[10] Brown TM, Krishnamurthy K. Histology, Dermis; 2024.

[11] Zorina A, Zorin V, Isaev A, Kudlay D, Vasileva M, Kopnin P. Dermal Fibroblasts as the Main Target for Skin Anti-Age Correction Using a Combination of Regenerative Medicine Methods. Current Issues in Molecular Biology. 2023 5;45(5):3829-47.

[12] Lynch B, Pageon H, Le Blay H, Brizion S, Bastien P, Bornschlögl T, et al. A mechanistic view on the aging human skin through ex vivo layer-by-layer analysis of mechanics and microstructure of facial and mammary dermis. Scientific Reports. 2022 1;12(1):849.

[13] Gerasymchuk M, Robinson GI, Kovalchuk O, Kovalchuk I. Modeling of the

Senescence-Associated Phenotype in Human Skin Fibroblasts. International Journal of Molecular Sciences. 2022 6;23(13):7124.

[14] Ogrunc M, d'Adda di Fagagna F. Never-ageing cellular senescence. European journal of cancer (Oxford, England : 1990). 2011 7;47(11):1616-22.

[15] Campisi J, d'Adda di Fagagna F. Cellular senescence: when bad things happen to good cells. Nature reviews Molecular cell biology. 2007 9;8(9):729-40.

[16] Emmetsberger Jaime. Reversing skin aging through senescence modulation. nature portfolio.

[17] Zhang L, Pitcher LE, Prahalad V, Niedernhofer LJ, Robbins PD. Targeting cellular senescence with senotherapeutics: senolytics and senomorphics. The FEBS Journal. 2023 3;290(5):1362-83. Available from: `https://febs.onlinelibrary.wiley.com/doi/10.1111/febs.16350`.

[18] Xu Z, Teixeira MT. The many types of heterogeneity in replicative senescence. Yeast. 2019 11;36(11):637-48.

[19] Sheekey Eleanor. My 1st science article - p53 & senescence!!. Youtube; 2022.

[20] Freund A, Laberge RM, Demaria M, Campisi J. Lamin B1 loss is a senescence-associated biomarker. Molecular Biology of the Cell. 2012 6;23(11):2066-75.

[21] Matias I, Diniz LP, Damico IV, Araujo APB, Neves LdS, Vargas G, et al. Loss of lamin-B1 and defective nuclear morphology are hallmarks of astrocyte senescence in vitro and in the aging human hippocampus. Aging Cell. 2022 1;21(1).

[22] Wang AS, Ong PF, Chojnowski A, Clavel C, Dreesen O. Loss of lamin B1 is a biomarker to quantify cellular senescence in photoaged skin. Scientific Reports. 2017 11;7(1):15678.

[23] Valieva Y, Ivanova E, Fayzullin A, Kurkov A, Igrunkova A. Senescence-Associated β-Galactosidase Detection in Pathology. Diagnostics (Basel, Switzerland). 2022 9;12(10).

[24] Campisi J ea Goberdhan P Dimri. A biomarker that identifies senescent human cells in culture and in aging skin in vivo. Cell Biology. 1995 9;92:9363-7.

[25] Lee BY, Han JA, Im JS, Morrone A, Johung K, Goodwin EC, et al. Senescence-associated β-galactosidase is lysosomal β-galactosidase. Aging Cell. 2006 4;5(2):187-95.

[26] Nagana Gowda GA, Abell L, Lee CF, Tian R, Raftery D. Simultaneous Analysis of Major Coenzymes of Cellular Redox Reactions and Energy Using ex Vivo ¹ H NMR Spectroscopy. Analytical Chemistry. 2016 5;88(9):4817-24.

[27] Wiley CD, Campisi J. The metabolic roots of senescence: mechanisms and opportunities for intervention. Nature metabolism. 2021 10;3(10):1290-301.

[28] Strømland Diab J, Ferrario E, Sverkeli LJ, Ziegler M. The balance between NAD+ biosynthesis and consumption in ageing. Mechanisms of Ageing and Development. 2021 10;199:111569.

[29] McReynolds MR, Chellappa K, Baur JA. Age-related NAD+ decline. Experimental gerontology. 2020 2;134:110888.

[30] Schultz MB, Sinclair DA. Why NAD(+) Declines during Aging: It's Destroyed. Cell metabolism. 2016 6;23(6):965-6.

[31] Wiley CD, Velarde MC, Lecot P, Liu S, Sarnoski EA, Freund A, et al. Mitochondrial Dysfunction Induces Senescence with a Distinct Secretory Phenotype. Cell Metabolism. 2016 2;23(2):303-14.

[32] Brinckerhoff CE, Matrisian LM. Matrix metalloproteinases: a tail of a frog that became a prince. Nature Reviews Molecular Cell Biology. 2002 3;3(3):207-14.

[33] Dasgupta J, Kar S, Liu R, Joseph J, Kalyanaraman B, Remington SJ, et al. Reactive oxygen species control senescence-associated matrix metalloproteinase-1 through c-Jun-N-terminal kinase. Journal of cellular physiology. 2010 10;225(1):52-62.

[34] Yuan X, Liu Y, Bijonowski BM, Tsai AC, Fu Q, Logan TM, et al. NAD+/NADH redox alterations reconfigure metabolism and rejuvenate senescent human mesenchymal stem cells in vitro. Communications Biology. 2020 12;3(1):774.

[35] Morsczeck C, Reck A, Reichert TE. Changes in AMPK activity induces cellular senescence in human dental follicle cells. Experimental Gerontology. 2023 2;172:112071.

[36] Debacq-Chainiaux F, Erusalimsky JD, Campisi J, Toussaint O. Protocols to detect senescence-associated beta-galactosidase (SA-βgal) activity, a biomarker of senescent cells in culture and in vivo. Nature Protocols. 2009 12;4(12):1798-806.

[37] Liu Cf, Li Xl, Zhang Zl, Qiu L, Ding Sx, Xue Jx, et al. Antiaging Effects of Urolithin A on Replicative Senescent Human Skin Fibroblasts. Rejuvenation Research. 2019 6;22(3):191-200.

[38] Wasiluk A, Waszkiewicz N, Szajda SD, Wojewódzka-Żelezniakowicz M, Kępka A, Minarowska A, et al. Alpha fucosidase and beta galactosidase in serum of a Lyme disease patients as a possible marker of accelerated senescence — a preliminary study. Folia Histochemica et Cytobiologica. 2012 7;50(2):270-4.

[39] Cahu J, Sola B. A sensitive method to quantify senescent cancer cells. Journal of visualized experiments : JoVE. 2013 8;(78).

[40] Neri F, Takajjart SN, Lerner CA, Desprez PY, Schilling B, Campisi J, et al. A Fully-Automated Senescence Test (FAST) for the high-throughput quantification of senescence-associated markers. bioRxiv : the preprint server for biology. 2024 3.

[41] Covarrubias AJ, Kale A, Perrone R, Lopez-Dominguez JA, Pisco AO, Kasler HG, et al. Senescent cells promote tissue NAD+ decline during ageing via the activation of CD38+ macrophages. Nature metabolism. 2020 11;2(11):1265-83.

[42] Shi B, Amin A, Dalvi P, Wang W, Lukacs N, Kai L, et al. Heavy-chain antibody targeting of CD38 NAD+ hydrolase ectoenzyme to prevent fibrosis in multiple organs. Scientific Reports. 2023 12;13(1):22085.

[43] Tarragó MG, Chini CCS, Kanamori KS, Warner GM, Caride A, de Oliveira GC, et al. A Potent and Specific CD38 Inhibitor Ameliorates Age-Related Metabolic Dysfunction by Reversing Tissue NAD+ Decline. Cell Metabolism. 2018 5;27(5):1081-95.

[44] Li Y, Liu Y, Zhang Y, Wu Y, Xing Z, Wang J, et al. Discovery of a First-in-Class CD38 Inhibitor for the Treatment of Mitochondrial Myopathy. Journal of Medicinal Chemistry. 2023 9;66(18):12762-75.

[45] Kawano Y, Kushima S, Hata H, Matsuoka M. The Role of CD38 in Multiple Myeloma Cell Biology. Blood. 2021 11;138(Supplement 1):1580-0.

[46] Qiu Z, Jia J, Zou H, Ao Y, Liu B, Wang Z. Targeting senescent cell clearance: An approach to delay aging and age-associated disorders. Translational Medicine of Aging. 2021;5:1-9.

[47] Peclat TR, Thompson KL, Warner GM, Chini CCS, Tarragó MG, Mazdeh DZ, et al. CD38 inhibitor 78c increases mice lifespan and healthspan in a model of chronological aging. Aging cell. 2022 4;21(4):e13589.

[48] Panche AN, Diwan AD, Chandra SR. Flavonoids: an overview. Journal of nutritional science. 2016;5:e47.

[49] Banjarnahor SDS, Artanti N. Antioxidant properties of flavonoids. Medical Journal of Indonesia. 2015 1;23(4):239-44.

[50] Ho CT. Antioxidant Properties of Plant Flavonoids. In: Food Factors for Cancer Prevention. Tokyo: Springer Japan; 1997. p. 593-7.

[51] Kim HP, Son KH, Chang HW, Kang SS. Anti-inflammatory Plant Flavonoids and Cellular Action Mechanisms. Journal of Pharmacological Sciences. 2004;96(3):229-45.

[52] Maleki SJ, Crespo JF, Cabanillas B. Anti-inflammatory effects of flavonoids. Food Chemistry. 2019 11;299:125124.

[53] Domaszewska-Szostek A, Puzianowska-Kuźnicka M, Kuryłowicz A. Flavonoids in Skin Senescence Prevention and Treatment. International journal of molecular sciences. 2021 6;22(13).

[54] Zhu Y, Tchkonia T, Pirtskhalava T, Gower AC, Ding H, Giorgadze N, et al. The Achilles' heel of senescent cells: from transcriptome to senolytic drugs. Aging Cell. 2015 8;14(4):644-58.

[55] Zoico E, Nori N, Darra E, Tebon M, Rizzatti V, Policastro G, et al. Senolytic effects of quercetin in an in vitro model of pre-adipocytes and adipocytes induced senescence. Scientific Reports. 2021 12;11(1):23237.

[56] Özsoy Gökbilen S, Becer E, Vatansever HS. Senescence-mediated anticancer effects of quercetin. Nutrition Research. 2022 8;104:82-90.

[57] Sohn EJ, Kim JM, Kang SH, Kwon J, An HJ, Sung JS, et al. Restoring Effects of Natural Anti-Oxidant Quercetin on Cellular Senescent Human Dermal Fibroblasts. The American Journal of Chinese Medicine. 2018 1;46(04):853-73.

[58] Lim H, Park H, Kim HP. Effects of flavonoids on senescence-associated secretory phenotype formation from bleomycin-induced senescence in BJ fibroblasts. Biochemical Pharmacology. 2015 8;96(4):337-48.

[59] Thakurdesai PA, Deshpande PO, Pore MP. Characterization, Preclinical Efficacy and Toxicity Evaluations of Flavonoids Glycosides based Standardized Fenugreek Seed Extract (FEFLG). Pharmacognosy Journal. 2023 3;15(1):90-105.

[60] Cristofalo VJ, Allen RG, Pignolo RJ, Martin BG, Beck JC. Relationship between donor age and the replicative lifespan of human cells in culture: A reevaluation. Proceedings of the National Academy of Sciences. 1998 9;95(18):10614-9.

[61] Kuehnemann C, Hu KQ, Butera K, Patel SK, Bons J, Schilling B, et al. Extracellular Nicotinamide Phosphoribosyltransferase Is a Component of the Senescence-Associated Secretory Phenotype. Frontiers in Endocrinology. 2022 7;13.

[62] Nacarelli T, Lau L, Fukumoto T, Zundell J, Fatkhutdinov N, Wu S, et al. NAD+ metabolism governs the proinflammatory senescence-associated secretome. Nature Cell Biology. 2019 3;21(3):397-407.

[63] Dreesen O, Chojnowski A, Ong PF, Zhao TY, Common JE, Lunny D, et al. Lamin B1 fluctuations have differential effects on cellular proliferation and senescence. Journal of Cell Biology. 2013 3;200(5):605-17.

[64] Kirkland JL, Tchkonia T. Senolytic drugs: from discovery to translation. Journal of internal medicine. 2020 11;288(5):518-36.

[65] Choi MH, Shin HJ. Anti-Melanogenesis Effect of Quercetin. Cosmetics. 2016 5;3(2):18.

[66] Upadhyay PR, Ho T, Abdel-Malek ZA. Participation of keratinocyte- and fibroblast-derived factors in melanocyte homeostasis, the response to UV, and pigmentary disorders. Pigment cell & melanoma research. 2021 7;34(4):762-76.

[67] Wu W, Yang B, Qiao Y, Zhou Q, He H, He M. Kaempferol protects mitochondria and alleviates damages against endotheliotoxicity induced by doxorubicin. Biomedicine & Pharmacotherapy. 2020 6;126:110040.

[68] Merecz-Sadowska A, Sitarek P, Kucharska E, Kowalczyk T, Zajdel K, Cegliński T, et al. Antioxidant Properties of Plant-Derived Phenolic Compounds and

Their Effect on Skin Fibroblast Cells. Antioxidants (Basel, Switzerland). 2021 5;10(5).

A

Appendix 1

A.1 Table: SA-β-Gal results

Table A.1: Percentage [%] of SA-β-Gal positive cells in high and low passage from three donors.

	Donor 1439		Donor 967		Donor 4081903.2	
Sample	**high**	**low**	**high**	**low**	**high**	**low**
1	33.5	9.81	44.2	2.78	65.8	6.67
2	33.1	24.1	35.4	11.3	57.3	18.1
3	A.3	B.3	41.2	14.2	71.7	8.82
4	A.4	B.4	36.9	4.02	E.4	F.4
5	A.5	B.5	57.5	6.4	E.5	F.5
6	A.5	B.5	45.8	7.89	E.5	F.5
Average [%]	33.3	16.9	43.5	7.8	48.7	8.4

A.2 Table: C12FDG results

Table A.2: Raw Data Cell Population for all samples of Low and High Passage Cells, from one donor.

Total population:	**Low**	**High**
Sample 1	905	112
Sample 2	1124	97
Sample 3	31	153
Sample 4	815	176
Sample 5	1021	115
Sample 6	1079	105
Sample 7	1083	173
Sample 8	849	45

Table A.3: Raw Data Intensity [GFP 469,525] for all samples of Low and High Passage Cells, from one donor.

Total Intensity:	**Low**	**High**
Sample 1	42135348	77032377
Sample 2	54935411	8907897
Sample 3	10812	11209172
Sample 4	11837950	66088550
Sample 5	95560869	20365267
Sample 6	51497072	5196518
Sample 7	75563699	19086194
Sample 8	85591811	2061676

DEPARTMENT OF LIFE SCIENCE
CHALMERS UNIVERSITY OF TECHNOLOGY
Gothenburg, Sweden
www.chalmers.se

CHALMERS
UNIVERSITY OF TECHNOLOGY